We are IntechOpen,
the world's leading publisher of
Open Access books
Built by scientists, for scientists

6,900
Open access books available

186,000
International authors and editors

200M
Downloads

154
Countries delivered to

Our authors are among the

TOP 1%
most cited scientists

12.2%
Contributors from top 500 universities

Interested in publishing with us?
Contact book.department@intechopen.com

Group III-Nitrides and Their Hybrid Structures for Next-Generation Photodetectors

Deependra Kumar Singh, Basanta Kumar Roul,
Karuna Kar Nanda and Saluru Baba Krupanidhi

Abstract

In the last few decades, there has been a phenomenal rise and evolution in the field of III–Nitride semiconductors for optoelectronic applications such as lasers, sensors and detectors. However, certain hurdles still remain in the path of designing high-performance photodetectors (PDs) based on III-Nitride semiconductors considering their device performance. Recently, a lot of progress has been achieved in devices based on the high quality epilayers grown by molecular beam epitaxy (MBE). Being an ultra-high vacuum environment based-technique, MBE has enabled the realization of high-quality and highly efficient PDs which have exhibited competitive figures of merit to that of the commercial PDs. Moreover, by combining the novel properties of 2D materials with MBE-grown III-Nitrides, devices with enhanced functionalities have been realized which would pave a way towards the next-generation photonics. In the current chapter, the basic concepts about photodetection have been presented in detail, followed by a discussion on the basic properties of the III-Nitride semiconductors, and the recent advancements in the field of MBE-grown III-Nitrides-based PDs, with an emphasis on their hybrid structures. Finally, an outlook has been provided highlighting the present shortcomings as well as the unresolved issues associated with the present-day devices in this emerging field of research.

Keywords: group III-nitrides, molecular beam epitaxy, photodetectors, hybrid structures, next-generation photonic devices

1. Introduction

Photodetectors (PDs) are the photonic devices that convert an incoming light signal into an output electrical signal. High-performance PDs are crucial for the advancements in the industrial and scientific communities, and these are being extensively used in areas such as video imaging, space and optical communications, flame detection, photovoltaic applications, environmental monitoring, and so on [1–5]. Some of the most extensively employed inorganic semiconductors for the development of PDs are zinc oxide (ZnO) [6], gallium arsenide (GaAs) [7], indium gallium antimonide (InGaSb) [8], germanium silicide (GeSi) [9] and gallium oxide (Ga_2O_3) [10], due to their excellent electronic properties like high charge carrier mobility and high light absorption coefficients. However, large exciton binding energies, low values of responsivity, slower response and narrow-band detection are some

of the major downsides associated with these materials [11]. Moreover, the synthesis as well as post-processing steps in the fabrication of antimony and arsenic-based devices involves toxic precursors as well as products, which are extremely hazardous for human health and for the environment as well. Thus, the quest is on for the development of high-performance PDs consisting of environment-friendly constituents.

The recent developments in the III-Nitride semiconductors-based devices have made a tremendous impact upon a number of technological areas such as information storage, lighting and full color displays, underwater and space communications, high-power and high-frequency electronic devices, photovoltaics, sensors and detectors, and so on [12–15]. The wurtzite polytypes of indium nitride (InN), aluminum nitride (AlN), and gallium nitride (GaN) have proved to be excellent semiconductors for band gap engineering, due to formation of continuous range of alloys with direct and tunable band gaps in the range of 0.7 to 6.2 eV [16]. Therefore, their intrinsic physical and chemical properties along with intense technological efforts have made the realization of versatile and reliable detectors in the entire ultraviolet (UV)-visible–near infrared (NIR) spectrum.

In spite of the significant progresses, the growth of epitaxial group III-Nitride thin films for practical devices, having low defect densities, has always been a challenge due to the lack of availability of lattice matched substrates. As of now, among various epitaxial growth techniques for III-Nitrides, plasma assisted molecular beam epitaxy (PAMBE) has emerged as the most versatile and environment-friendly synthesis technique, involving low growth temperature, controlled growth rates which result into the formation of heterostructures with sharp interfaces, and non-hazardous precursors and by-products. Since pristine III-Nitride substrates are immensely costly and therefore, not yet available for research and industrial purposes, the development of this family of semiconductors proceeds entirely by the heteroepitaxial growth on various foreign substrates such as sapphire, Si (111) and 6H-SiC [16–18], and one has to often compromise with the device performance. It may be noted here that hybrid structures of III-Nitrides with other semiconductors such as ZnO, perovskites, and two-dimensional (2D) layered materials such as MoS_2 are expected to deliver competitive device performance as compared to the commercial PDs ([19–21]. In the forthcoming sections, we discuss about the figures of merit involved in the evaluation of a PD, followed by a brief overview of III-Nitrides and their properties. Then, a detailed analysis about the recent advancements in the MBE-grown III-Nitrides for photodetection application has been presented and finally, we wind up by discussing the unresolved difficulties and propose an outlook in this developing field of optoelectronics.

2. Basic concepts about photodetection

A PD is a sensor that detects an incoming electromagnetic radiation. Whenever light waves of energy greater than or equal to the band gap of a semiconductor are absorbed, there is an overall change in the conductivity of the semiconductor. Thus, PD is a device developed on the principle of this photoconducting effect and it quantifies the speed and the amplitude of the change in the conductivity, in respect of incoming electromagnetic radiations.

2.1 Important figures of merit of a PD

Several figures of merit and parameters are used for the evaluation of a PD, and these performance metrics allow us to compare various devices. Mostly, the output

electrical signal is recorded from the device and realized in the form of an output photocurrent, and thus, all the key figures of merit are defined in terms of this output photocurrent. The output photocurrent (I_P) is defined [11] as

$$I_P = I_{Illuminated} - I_{Dark} \qquad (1)$$

where $I_{Illuminated}$ is the output current detected upon light illumination and I_{Dark} is the dark current in the device (i.e. without any light illumination). Photocurrent can be enhanced by reducing the probability of recombination of photogenerated electrons and holes, and this can be achieved by fabricating high-quality and defect-free devices, using heterojunctions with type-II band alignment which result into the effective separation of charge carriers. Devices utilizing p-n junctions which operate in reverse bias, usually show a large photocurrent due to the enhanced carrier separation as well as lower dark current.

2.1.1 Responsivity

Responsivity (R_λ) is defined as the ratio of the photocurrent generated and the incident optical power of a specific wavelength on a predefined device area. It is given [11] by the following mathematical formula

$$R_\lambda = \frac{I_P}{P \times A} \qquad (2)$$

where P is the incident power density of light and A is the device area where light is being illuminated. Its units are AW^{-1}. It quantifies the extent of achievable electrical signal in a PD when illuminated by a light of certain power density. Thus, a larger responsivity signifies a larger electrical output signal for a specific optical excitation power. Replacing a single material-based or homojunction-based device with heterojunction-based devices with type-II band alignment is an effective way to enhance the responsivity due to minimized recombination of photogenerated electrons and holes [22]. Another approach is to promote devices which possess a strong built-in potential that supports the external electric field to enhance the carrier separation and transport [15]. Growth of high-quality crystals reduces the defect density present in the system, thereby suppressing the scattering and recombination of the charge carriers which enhances the responsivity of the device. Manohar et al. [6] recently demonstrated a highly cost effective and an elegant method to immensely enhance the photoresponsivity of a PD by suppressing the carrier recombination through coatings of different materials which facilitate either electron or hole transfer to the metal contacts.

2.1.2 Specific detectivity

A fundamental performance parameter for a PD is its specific detectivity, that measures the ability of a PD to detect weak light signals. For a PD, this metric can be defined in terms of the noise equivalent power (NEP). The NEP of a PD is proportional to the ratio of the square root of the dark current (I_{Dark}) to the responsivity (R_λ) of the PD at a given wavelength. It can be defined by the following relation:

$$NEP = \frac{\sqrt{(2 * e * I_{Dark})}}{R_\lambda} \qquad (3)$$

where e is the electronic charge. The specific detectivity (D^*) of a PD is defined as the ratio of the square root of the active area (A) to its NEP [4], and is given by the following equation

$$D^* = \frac{\sqrt{A}}{NEP} \qquad (4)$$

It is measured in Jones. Higher detectivity of a PD indicates that even a very weak signal can be detected. It may be noted that lower is the dark current, higher is the detectivity. PDs based on p-n junctions operated in the reverse bias generally exhibit very high specific detectivities because of low values of dark current.

2.1.3 Internal gain

The internal gain (G) of a PD refers to the number of electrons collected at the electrodes per incident photon. It can be determined [4] by the following relation

$$G = \frac{hc * R_\lambda}{\eta e \lambda} \qquad (5)$$

where h, c, η and λ are the Planck's constant, the velocity of light in vacuum, the EQE of the device and the illumination wavelength, respectively.

In other words, internal gain is the ratio of the hole carrier lifetime to the electron transit time and is given [4, 10] by

$$G = \tau/t \qquad (6)$$

where τ is the mean hole carrier lifetime and t is the electron transit time. So, high internal gains can be achieved by fabricating devices which exhibit high responsivities. Another approach to enhance gain is by trapping one kind of charge carrier (generally holes), so as to prevent it from recombination. Thus, the carrier lifetime of the holes increases and in turn gain increases.

2.1.4 Sensitivity

Sensitivity (S) of a PD is defined [23] as the ratio of the photocurrent to the dark current.

$$S = \frac{I_P}{I_{Dark}} \qquad (7)$$

Hence, sensitivity can be improved by either enhancing the value of photocurrent or lowering the dark current. The enhanced photocurrent can be achieved by fabricating high quality and defect-free interfaces and devices, thus, reducing the scattering effects of the photogenerated electrons and holes, and leading to higher photocurrents. Devices consisting of p-n junctions show ultralow values of dark currents exhibiting higher sensitivities.

2.1.5 Response/recovery time

An important aspect of a PD is how fast it detects the incident light, and how fast it comes back to its initial state once the incident light is removed. This is quantified by estimating the response/recovery times of the PD. Lower the values of

these time constants, faster is the detection process. Mukhokosi et al. [23] have demonstrated that the response times of a PD are controlled by the carrier mobilities of the constituent semiconductors of the PD. The transit time ($\tau_{transit}$) of a p-n heterojunction is given [23] by the following relation

$$\tau_{transit} = \frac{W}{v_{drift}} = \frac{W}{\mu_{drift} E_o} \tag{8}$$

where W is the depletion region width, μ_{drift} is the carrier mobility and E_o is the built-in electric field at the junction. Therefore, high-quality substrates with high carrier mobilities such as p-Si, usually result into very small response time. The depletion width can be narrowed down by fabricating highly doped p-n junctions, which in turn decreases the transit time in accordance with Eq. (8).

Other parameters that affect the response speed of a PD are the junction capacitance (C) and the series load resistance (R), and thus, the corresponding RC time constant. The rise time of a PD with an RC circuit is given by:

$$\tau_r \cong 2.2 RC \tag{9}$$

Therefore, decreasing the junction capacitance can further improve the response time. The junction capacitance depends on the width of the depletion layer, and smaller depletion widths increase the capacitance. Therefore, the width of the depletion region should be optimum to minimize the carrier transit time.

In addition, defect-free semiconductors exhibit faster response times, because of reduced recombination of the photogenerated carriers. For the case of linear devices, high-quality photosensitive materials as well as defect-free semiconductor/ electrode interfaces are required to minimize the carrier scattering and recombination processes, and result into the lowering of the carrier transit time.

2.1.6 Power consumption

One of the most critical parameters associated with a PD is its power consumption. Generally, PDs require an external power source as the driving force to separate the photogenerated electrons and holes efficiently. Thus, a lot of external energy is required in a system that consists of several such detectors. Therefore, it is a big concern in the present energy scenario. Hence, a lot of research is being focussed these days on achieving self-powered or zero-biased PDs [24, 25], which utilize a built-in electric potential for the effective charge carrier separation. The extensively used technique for fabricating self-powered PDs is by utilizing a p-n junction, where a strong electric field is created at the interface, and therefore, the device can operate in zero-bias mode.

2.1.7 Spectral range

Another crucial aspect of PDs is their detection range. PDs are generally classified into two categories based on their spectral range of detection: broad-band (which shows a considerable detection to a wide range of wavelengths) and narrow-band or wavelength-selective (whose detection range is very limited) PDs. The most common way to fabricate a wavelength-selective PD is by using a single semiconductor (of desired band gap) as the active material in the device. Another way to achieve wavelength selectivity is by integrating an optical microcavity within the PD. This optical microcavity consists of distributed Bragg reflectors (DBR), which allow multiple reflections of a specific wavelength. These reflections interfere

constructively, leading to increased light-matter interactions and result into the enhancement of photocurrent. This occurs only at the design wavelength of the cavity, whereas all the off-resonance wavelengths incident on the PD are rejected by the cavity. On the other hand, broad-band photodetection can be realized by making heterojunctions-based devices consisting of different semiconductors of appropriate band gaps, as demonstrated by Singh et al. [26] by making a hybrid device based on SnS_2/p-Si heterojunction, which shows a broad-band response in the entire ultraviolet to near infrared range. Usually, conventional PDs suffer from the trade-off between selective and broad-band detection. Recently, a few devices have been reported to exhibit a unique feature wavelength-selectivity in a broad-band spectral response, through the phenomenon of polarity switching [27, 28].

2.2 Different mechanisms of photodetection

PDs rely on distinct sensing mechanisms depending upon the intrinsic properties of the photosensitive materials used as well as the architecture of the device structures. We now briefly discuss the most commonly adopted sensing mechanisms.

2.2.1 Photoconductive and photogating effects

The photoconductive effect involves photogeneration of excess free carriers in a semiconductor material, when photons with energy higher than the band gap of the semiconductor are absorbed, which eventually leads to a change in its electrical conductivity. The photoconductive effect is the most primitive form of photodetection, where two Ohmic contacts are deposited on the semiconductor surface to form a metal–semiconductor–metal (MSM) type linear device configuration [29]. The schematic of a PD depicting the process of photoconduction is shown in **Figure 1(a)**. It is important to note that this change in conductivity is a result of the change in the free charge carrier concentration due to the photogeneration process. Thus, the effective spectral range of photoconductive PDs is limited by the band gap of the semiconducting material or the photoactive layer. Additionally, a photoconductive PD usually requires an externally applied voltage for the effective separation and the directional propagation of the photogenerated carriers. This generally results in relatively larger values of the dark current, which leads to a lower on/off ratio and higher energy consumption. Additionally, conventional photodiodes (non-linear devices) also work in the photoconductive mode when operated in the reverse bias condition.
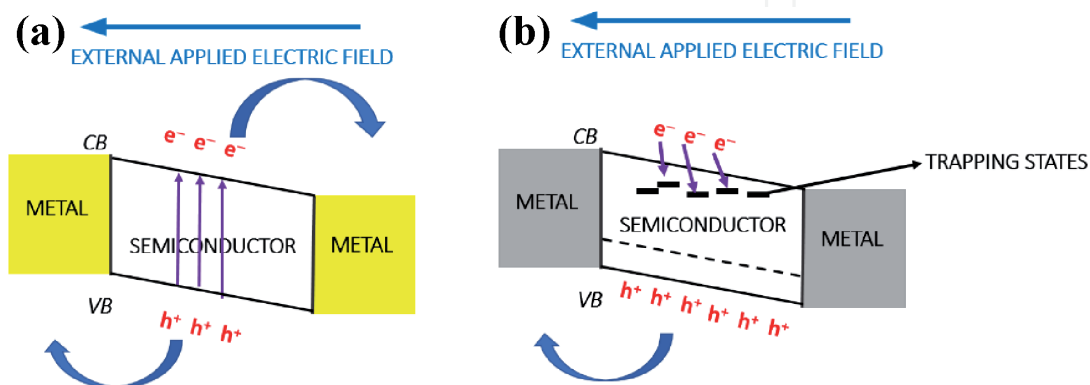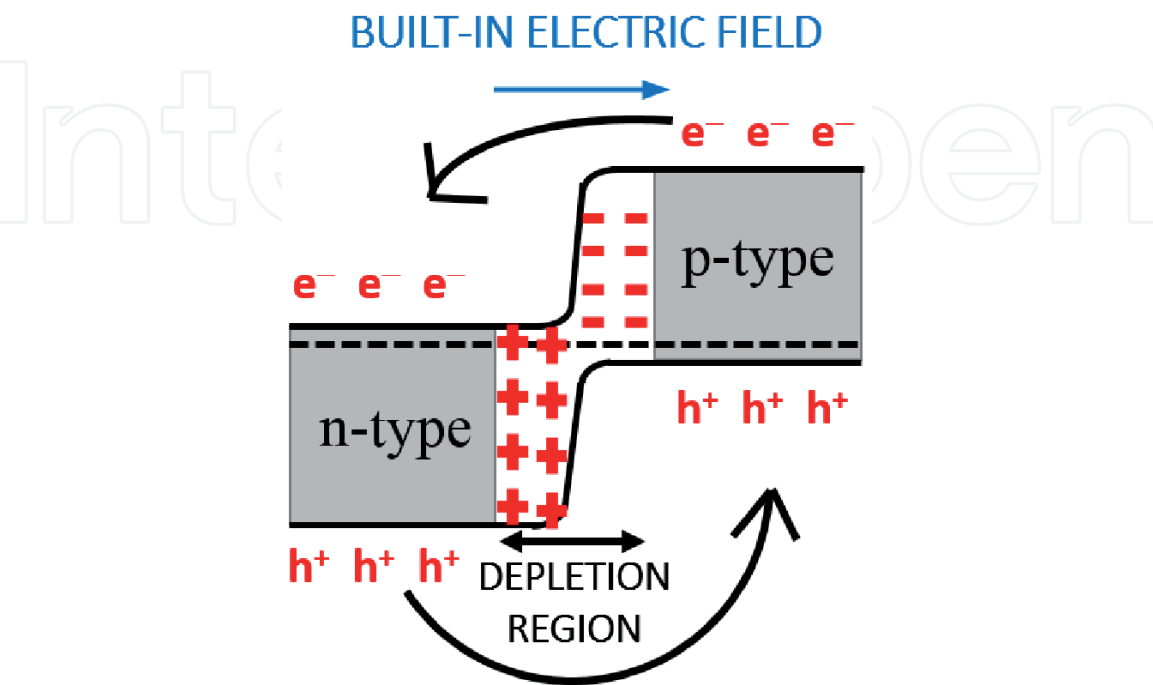

Figure 1.
Schematic view of (a) a photoconductor depicting the process of electron–hole pairs generation and their transport and (b) a PD based on the photogating effect under illumination. The defect states capture electrons which eventually modulates the conductivity of the material.

Photogating effect is a type of photoconducting effect, wherein certain localized states such as defects or surface states exist within the forbidden gap of the semiconductor. The effect normally originates when the photogenerated charge carriers are captured by the localized trapping states present within the system [30] as depicted in **Figure 1(b)**. This effect is pronounced in low-dimensional material systems such as 2D layered materials and quantum dots, which have very large surface-to-volume ratio and less screening in the z-direction. Since one type of charge carriers are trapped, it leads to prolonged carrier lifetimes, and therefore, PDs which exhibit the photogating effect usually show higher photogains. In addition, faster transit times and enhanced photocurrent is observed due to suppressed carrier recombination.

2.2.2 Photovoltaic effect

Photovoltaic effect is the phenomenon of spontaneous generation of a photocurrent upon light illumination in a PD. This effect is generally realized in p-n junction-based devices, where a built-in electric potential exists at the interface [31]. Upon light illumination, electrons and holes are created near the semiconductor interface. Under the influence of the existing built-in voltage, these electrons and holes get separated, thereby, causing a photocurrent to flow along the direction of this built-in potential (**Figure 2**). The photovoltaic effect is closely related to the photoelectric effect and therefore, the effective wavelength range is usually limited by the band gap of the constituent photosensitive material. However, in the case of p-n heterojunctions, due to the intimate energy band coupling that enables interband transition between different semiconductors, the effective detection range can be modulated beyond the limitation of the band gaps. The biggest advantage associated with PDs based on the photovoltaic effect is that due to the intrinsic built-in electric potential, the PDs do not require any external power for their operation [11]. Furthermore, the photovoltaic PDs possess low dark current under the zero-biased working mode, which is beneficial for the detector.

Figure 2.
Schematic depicting the photovoltaic effect.

2.2.3 Photothermoelectric effect

The origin of photothermoelectric (PTE) effect is the temperature gradient (ΔT) developed due to the thermal effects of the light illumination. Subsequently, a potential gradient (ΔV_{PTE}) is created that serves as the driving force for the transport of the photocurrent through the device (**Figure 3**). The thermoelectric voltage generated is given [32] by

$$\Delta V_{PTE} = S\Delta T \tag{10}$$

where S is Seebeck coefficient of the material [33]. PTE effect-based PDs can operate without external power, i.e. they are self-powered in nature. However, the thermoelectric potential created is very low, generally in the range of millivolts (mV) and microvolts (μV), which seriously limits the popularization and hence, wide scale applications of PTE-based PDs.
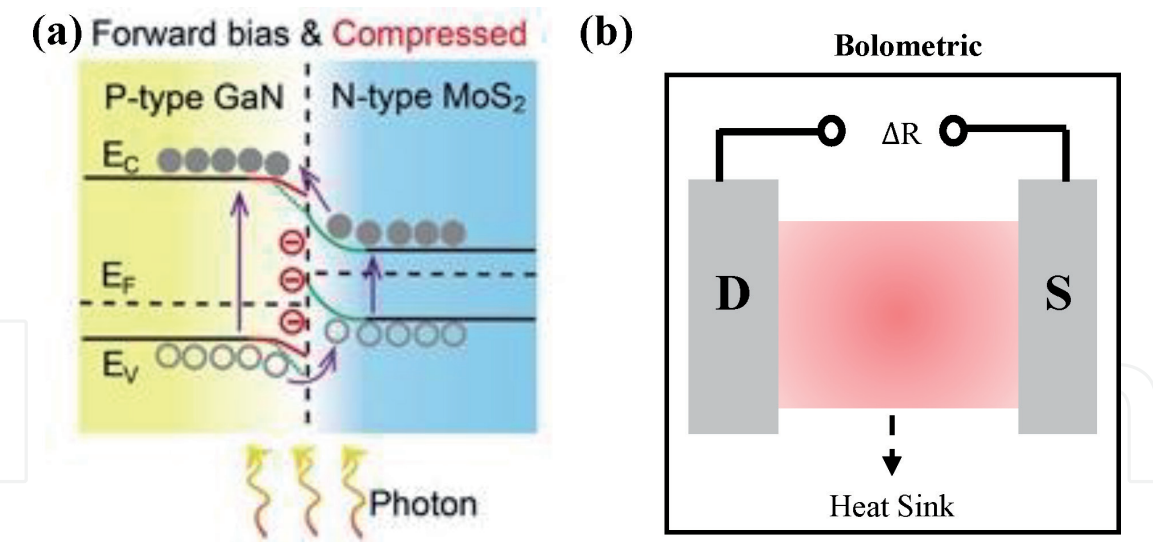
2.2.4 Piezophototronic effect

The devices that make use of the piezo-potential of the constituent materials for controlling the carrier generation and transport, for improving the overall performance of the opto-electronic devices are referred to as piezophototronic [32]. The basic requirement of such devices is a piezo-electric material such as ZnO, GaN, etc. which can produce an electric potential upon variations in the applied stress. The operational mechanism of a piezophototronic device is based upon the fundamental principles of the conventional Schottky contacts and p–n junctions. Ionic charges are introduced by the effect of piezoelectric polarization, which tune the charge transport at the junction. The effect of piezophototronicity on a p-n junction (GaN/MoS_2 in this case) under compressive strain is shown in **Figure 4(a)**. When the [0001]-oriented GaN film is under a compressive strain, negative piezopotential is produced inside GaN. This results into the lowering of the junction barrier. Therefore, more photogenerated charge carriers can cross the junction [34]. Hence, the photoresponsivity gets enhanced. An opposite effect (positive piezopotetial in GaN film, which increases the junction barrier) is observed in the case of applied tensile stress.

2.2.5 Photobolometric effect

Photobolometric effect is the alteration in the electrical resistance of a material, which is induced by the heating effect of uniform light illumination [32]. Typically, the active material layer absorbs the incident photons and then converts them into
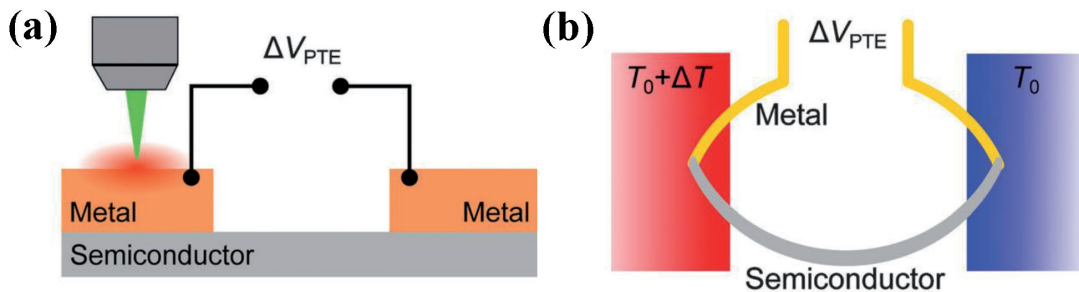
Figure 3.
(a) Schematic of a PTE based device illuminated locally by focused light. An open circuit voltage which is equal to the thermoelectric voltage ΔV_{PTE} gets developed across the electrodes. (b) Thermal circuit equivalent to the device depicted in (a). Figure is reproduced with permission from Ref. [33].

Figure 4.
(a) Piezophototronic enhancement observed in p-GaN/n-MoS$_2$ heterojunction. When the [0001]-oriented GaN film is compressed, negative piezoelectric charges develop in the GaN film near the interface, and the junction barrier gets lowered. This allows a greater number of carriers to pass through the junction. Figure is reproduced with permission from Ref. [34]. (b) Schematic depicting bolometric effect. The red shaded region indicates elevated temperature with the temperature gradient (ΔT) and ΔR denotes the resistance change across the channel. Figure is adapted from Ref. [35].

heat energy. The extent of this effect is proportional to the conductance change in the photoactive material with temperature (dG/dT) as well as the homogeneous temperature change (ΔT) induced by light illumination (**Figure 4(b)**). The change in conductance is influenced by change in the charge carrier mobility of the material because of the induced temperature change. Photobolometric effect generally occurs in the wavelength range of mid-infrared to far-infrared. Additionally, similar to PDs based on photoconductive effect, photobolometric PDs also require an external power source, which differentiates them from the PTE-based PDs.

3. Group III-Nitride semiconductors

From the early decades, silicon has been considered as one of the major components in the semiconductor industry because of its unique properties. Later, III-V materials, particularly the arsenic based compounds, gained much attention because of their superior properties such as high electron mobility, direct and tunable band gap, etc. The group III-Nitrides came into the picture around 1960s, and active research on this material system started with the development of blue light emitting diodes. Over the time, much of the attention of the researchers and scientists has been diverted on different classes of materials. However, group III-Nitride semiconductors continue to maintain their stronghold due to the exceptional properties and the unique advantages they offer.

3.1 Crystal structure and optical properties of group III-Nitrides

Group III-Nitride semiconductors, mainly comprising of AlN, GaN and InN, exist in three different crystal structures, namely, wurtzite, zincblende and rocksalt. Among these, the most stable and the lowest energy structure is the wurtzite system [36]. The wurtzite structure has a hexagonal unit cell and contains six atoms of each type, with space group P63mc. The wurtzite polytype is made up of two interpenetrating hexagonal close-packed unit cells, each containing one type

of atom, and with an offset along the c-axis by 5/8 of the cell height. The stacking sequence in the hexagonal structure consists of alternating hexagonal planes of group III and N atom, with a stacking sequence of ABAB [36]. A stick-and-ball model-based diagram of the hexagonal unit cell of III-Nitride semiconductors is shown in **Figure 5**. The group III semiconductors and the nitrogen atoms have been shown in different colors [37]. The polytypes of the III-Nitrides having wurtzite structure, form a continuous alloy system, with direct band gaps ranging from 0.7 eV for InN, 3.4 eV for GaN, and to 6.2 eV for AIN [16]. Therefore, the III-Nitrides are potential candidates for fabrication of optical devices which are active at wavelengths ranging from the NIR to the UV.

3.2 Growth of group III-Nitride semiconductors

The first successful synthesis of GaN dates back to as early as 1930s. In 1969, Maruska and Tietjen [38] synthesized single crystalline GaN layers on sapphire substrates by using the technique of hydride vapor phase epitaxy (HVPE). Although most of the III-Nitride semiconductors, especially for industrial-scale production, are usually synthesized via metal–organic chemical vapor deposition (MOCVD), metal–organic vapor phase epitaxy (MOVPE) and HVPE, however, these techniques have some serious drawbacks associated with them. These fabrication methods are generally characterized by quite high growth temperatures (>900°C). Thus, the sample is subjected to a high level of stress when cooled down to the room temperature from such high temperatures. Moreover, the inevitability of such high temperatures has hindered the growth of high-quality InN and its alloys, which are potential candidates for IR and terahertz (THz) optoelectronic applications, due to the dissociation of InN at such high temperatures [16]. There are also various other less-known techniques used for the synthesis of the group III-Nitrides, which are derivatives of the above three methods. However, all these processes involve the treatment and usage of toxic precursors as by-products, and therefore, making


Group III Element   **Nitrogen**
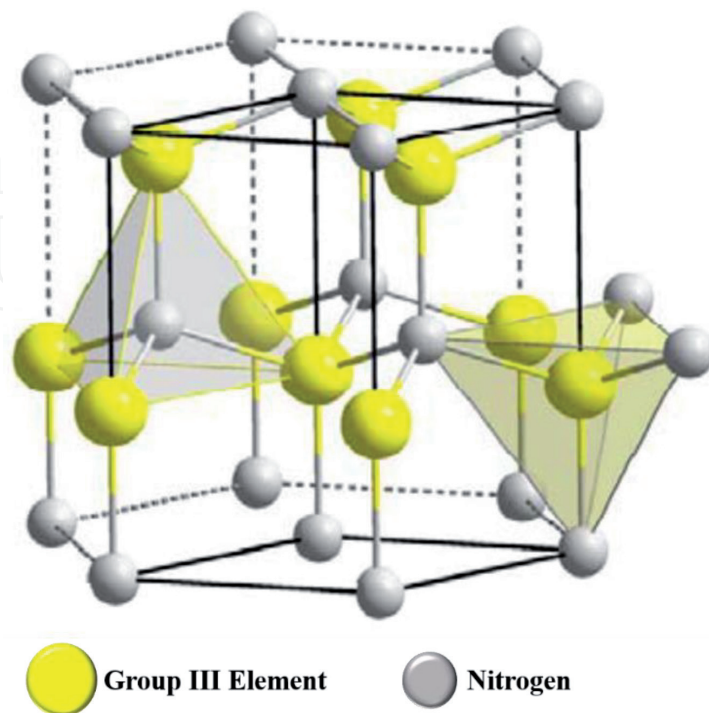
Figure 5.
The wurtzite crystal structure of III-nitrides. Nitrogen and group III atoms are represented by gray and yellow spheres, respectively. Figure has been reproduced with permission from Ref. [37].

these techniques less environment-friendly and hazardous to human health, which has become a major concern at the global level.

PAMBE, on the other hand, is a much cleaner synthesis technique and offers the advantage of fabrication of better-quality samples, along with a very important benefit of growth at much lower substrate temperatures when compared with most of its counterparts. MBE is an epitaxial and layer-by-layer growth technique involving precise control of the supply of thermally evaporated atomic species (**Figure 6(a)**). This results into construction of 2D layers on a substrate by means of lattice matching (**Figure 6(b)**). The major advantages of MBE are that it is clean, scalable and highly controlled with a high product quality. The involvement of ultra-high vacuum growth environment and the use of ultra-high purity elements as the source materials, minimize the inclusion of contaminants and impurities in the grown structures. Additionally, with the advent of higher growth rate RF-plasma
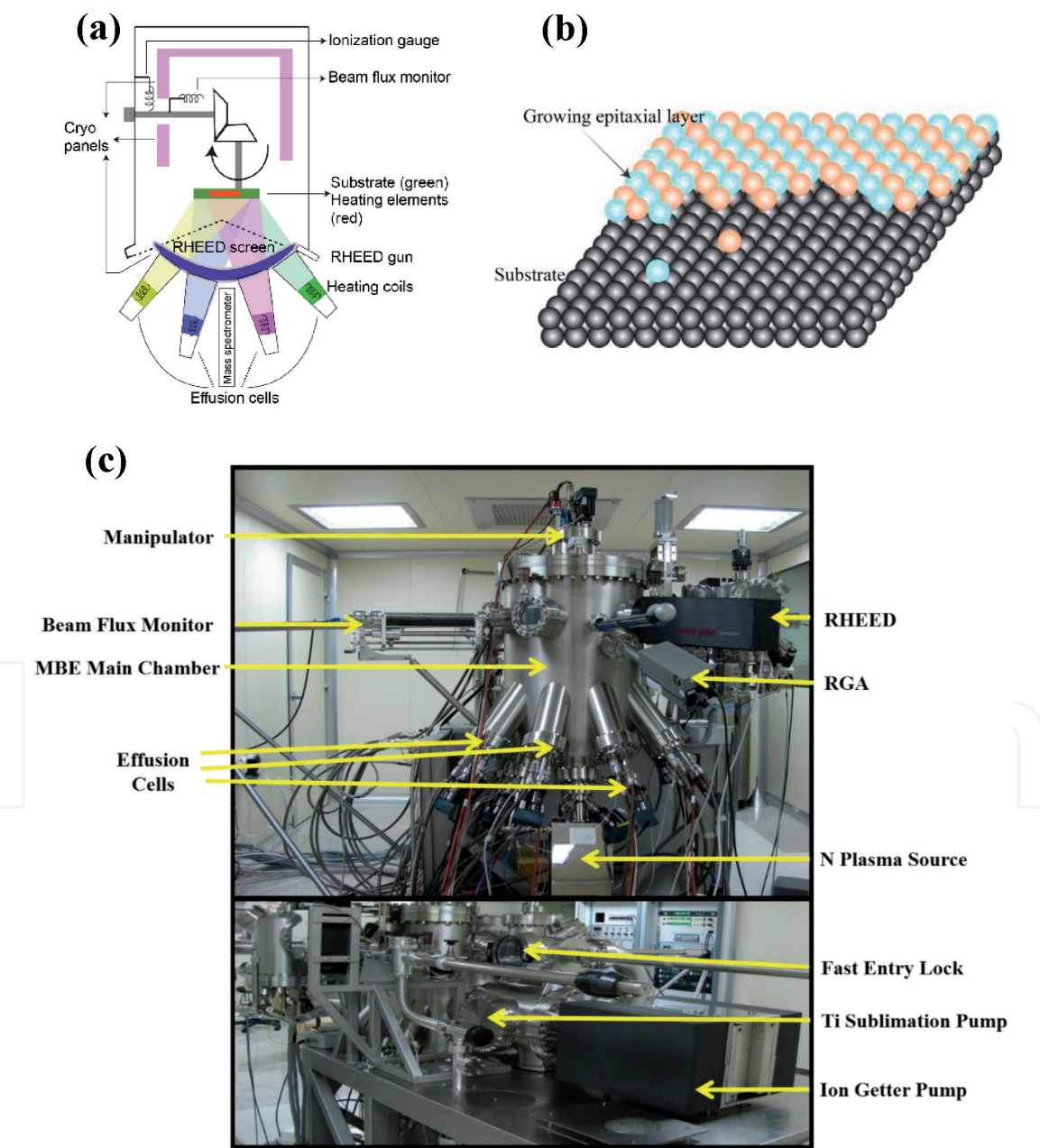
Figure 6.
(a) Schematic of a typical MBE system, showing various components. Figure has been adapted with permission from Ref. [40]. (b) Schematic depicting epitaxial growth of a material on a substrate. (c) MBE system located in materials research Centre, Indian Institute of Science, Bangalore, India.

sources, the synthesis times have been significantly reduced without compromising in the structural quality. One of the earliest works demonstrating growth of GaN by MBE was reported by Yoshida et al. [39] in 1983, wherein they successfully synthesized high electrical and optical quality GaN thin films on sapphire, with an AlN buffer layer via reactive MBE using ammonia as nitrogen source. **Figure 6(c)** shows the MBE setup located in Materials Research Centre, Indian Institute of Science, Bangalore, India.

3.3 Approaches to improve device performance of group III-Nitride semiconductors-based PDs

Researchers across the world have employed various approaches to improve the performance of the III-Nitrides-based devices. These include improvement in growth quality by the employment of different growth techniques, adopting novel growth methods like epitaxial lateral overgrowth (ELO), using different materials as buffer layers such as AlN, and by fabricating improved structures to reduce defects. Another way to improve the growth quality of III-Nitrides is to find the alternatives to conventional silicon and sapphire substrates. In this regard, transition metal dichalcogenides, having a small lattice mismatch with III-Nitrides, can be used as potential substrates. Engineering the device structures can also result into the improvement of the device performance, and this can be achieved by making quantum confinement architectures, and by making hybrid structures using 2D materials like graphene and MoS_2.

## 4. Recent advancements in the MBE grown III-Nitrides-based PDs

In the preceding sections, we have focused on the important figures of merit of PDs along with the different mechanisms of photodetection, and the properties and growth methods for group III-Nitride-based devices. Numerous reports exist which demonstrate the photodetection properties of III-Nitrides-based PDs. The recent state-of-the-art III-Nitride-based PDs have been discussed wherein a special emphasis on self-powered photodetection has been given.

4.1 III-Nitrides-based devices

Some early accomplishments in the field of GaN-based PDs grown by MBE have been achieved by several researchers such as Van Hove et al. [41], Son et al. [42], Torvik et al. [43], Osinsky et al. [44], Xu et al. [45], and so on. In 2005, Calarco et al. [46] reported the electrical transport of GaN nanowhiskers grown by MBE, in dark and under UV illumination. The photoresponse has been found to be sensitively dependent on the column diameter of the nanowhiskers and this effect has been quantitatively described through a mechanism of size dependent surface recombination. Jain et al. [47] have shown the effect of symmetric and asymmetric contact electrodes on *c*-GaN/sapphire based UV PD. In 2018, Goswami et al. [48] reported the growth of self-assembled GaN nanostructures on Si(111) for applications in UV photodetection (**Figure 7**). The device exhibited a responsivity of 5.7 mAW^{-1} at a bias of 1 V. Numerous other reports exist demonstrating the photodetection properties of GaN-based PDs.

In the meantime, researchers have also started exploring InN-based devices. One such work has been carried out by Shetty et al. [49]. They have grown InN quantum dots of varying densities on Si substrates using MBE. The device shows a strong response towards infrared illumination. The photoresponse studies revealed that
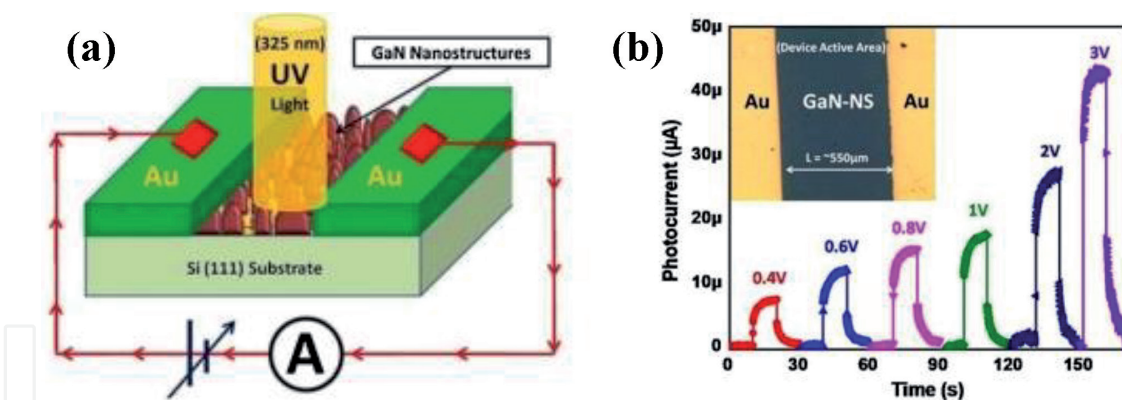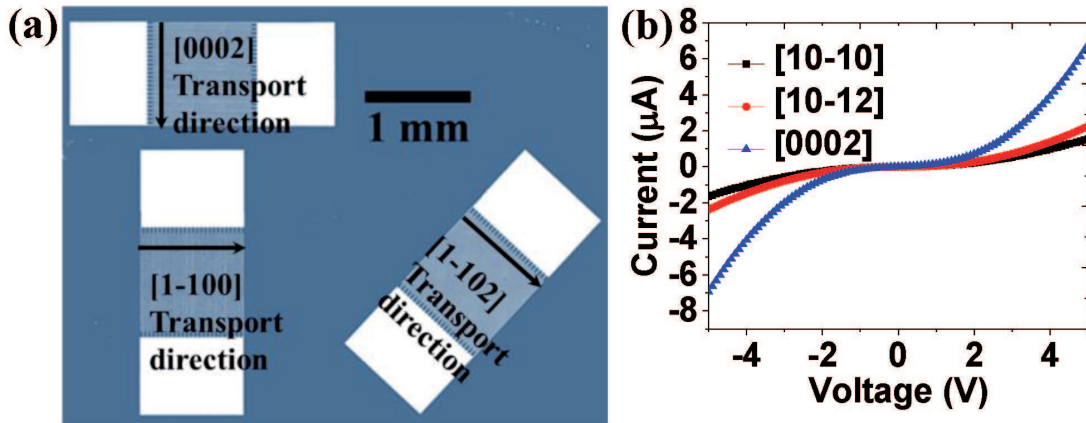
Figure 7.
(a) Schematic of the fabricated MSM device and (b) trend of photocurrent variation with respect to the applied bias. Inset shows the optical image of the actual PD. Figure has been reprinted with permission from Ref. [48].

the increasing dot density results in the improvement in the sensitivity of the PD. The increase in the photocurrent with the density of the quantum dots has been attributed to the increase in the number of photogenerated carriers in InN, which add up with the carriers generated in Si upon light illumination. The results have also been validated using simulations and it has been observed that the experimental as well as theoretical results have sufficient agreement between them.

However, the epitaxial growth of high-quality III-Nitrides has been always hindered by the lack of lattice-matched substrates, that hinders the development of high-performance devices. In all the above-mentioned reports, the growth has been accomplished on substrates (*c*-plane sapphire, Si(111), etc) which promote the *c*-plane oriented growth of the III-Nitrides i.e., in the polar direction. Moreover, the structures grown along the polar *c*-axis exhibit larger internal electric fields at the heterostructure interfaces, affecting the radiative recombination rates. To overcome these issues, non-polar III-Nitrides are being extensively explored now-a-days because of their several benefits over the polar III-Nitrides. Epitaxial growth of GaN in the non-polar (*a*-plane) direction seems to be a feasible way for the growth of high-quality films as the lattice mismatch between *a*-plane [11–20] GaN and the *r*-plane [1–102] sapphire is the least (1.19%) along one of the azimuth directions. Additionally, the absence of internal polarization fields in non-polar structures may enhance the photodetection performance. Mukundan et al. [50] in 2015 have shown improvement in the performance of non-polar GaN in comparison to that of the polar GaN in terms of figures of merit as well as the device stability.

In 2018, the mechanism of the higher device performance parameters of the non-polar GaN has been explained by Pant et al. [18] by performing azimuth angle-dependent photodetection. They have shown the non-uniformity in the defects present along the different azimuth directions. This is a consequence of the asymmetry in the strain between the substrate and film, as the lattice mismatch is asymmetric along various in-plane crystal directions. The mismatch in the lattice constants along the [0002] direction is ~1% whereas, along the [1–100] direction, it is ~13%. This induces a large number of defects along the [1–100] direction as compared to the [0002] azimuth direction. **Figure 8(a)** shows the *a*-GaN-based device used in this study. Furthermore, it has been shown in **Figure 8(b)** that the overall photocurrent in the UV region is also dependent on the different azimuth angles. A maximum responsivity of ~1.9 AW^{-1} and ~ 13.0 AW^{-1} have been obtained at a bias of 1 V and 5 V, respectively. These results underlined the importance of aligning the contact electrodes along the favorable azimuth direction in order to restrict the transport of the charge carriers. In a subsequent work, Pant et al. [51] have further shown

Figure 8.
(a) Fabrication of contact electrodes in different directions and (b) I–V characteristics of the device taken along different azimuth directions. Figure has been reprinted with permission from Ref. [18].

improvements in the photodetection properties of the non-polar GaN by optimizing the growth parameters and therefore, improving the overall quality of the thin film. A maximum responsivity of 25 AW^{-1} has been achieved at a low bias of 1 V and is among the highest reported responsivities at such low voltages.

Another approach to overcome the problem of lattice mismatch is by using AlN as a buffer layer. Wang et al. [52] in 2007 exhibited a Schottky-based metal–semi-conductor–metal PD, fabricated on 1 μm-thick and crack-free GaN on Si(111), utilizing an optimized $Al_xGa_{1-x}N$/AlN complex buffer layer. The device showed a high photoresponsivity of 4600 AW^{-1} at 1 V bias (366 nm) and this superior performance has been attributed to both the crack-free GaN film as well as the high internal gain. In another report, the growth of GaN p-n junction on AlN/Si(111) and the effects of thermal annealing of the Ni/Ag contact electrodes on the photo-detector applications have been explored by Yusoff et al. [14]. Recently, Ravikiran et al. [53] have demonstrated GaN UV PDs grown on AlN/Si(111) which exhibited a peak responsivity of 0.183 AW^{-1} at 15 V.

4.2 III-Nitride heterostructures-based devices

In the reports discussed above, various methods leading to enhancement in the responsivity have been highlighted. However, the responsivities and the transit times (in the order of a ms) of most of these PDs still remain inferior to that of the state-of-the-art detectors, and therefore, hamper their usage for the design and development of practical devices. The most elegant way to enhance the device performance is by utilizing a heterojunction with high-quality materials. There are many reports demonstrating PDs based on the heterojunctions of III-Nitrides with other III-Nitride semiconductors, ZnO, perovskites, 2D materials, and so forth.

In 2010, Rigutti et al. [54] have shown a single-nanowire PD relying on the charge carrier generation in the GaN/AlN quantum discs (QDs). The photolumi-nescence studies have shown that the emission energy of the QDs is lesser than the band gap of GaN, which is a consequence of the quantum confined Stark effect. The QD-based PDs exhibited a strong reduction in the dark current with responsivity (300 nm, −1 V) as high as 2×10^3 AW^{-1}. Yusoff et al. [55] have demonstrated AlN/GaN/AlN heterostructures grown via PAMBE on Si substrates. The photoresponse shows promising results towards applications in UV detection. Pandey et al. [21] have reported the fabrication of a $BaTiO_3$/GaN (BTO/GaN)-based Schottky junc-tion PD on *c*-plane sapphire and its selective UV photodetection in temperature range of 313–423 K. The responsivity increased with increase in the temperature till

393 K and then it decreased. Such behavior has been explained by the enhancement in the device's dark current with increase in the temperature, which is also evident from the ideal diode equation. The device shows potential to be used as an UV PD in high-temperature applications.

In another report, Roul et al. [13] have demonstrated hybrid ZnO/AlN/Si-based UV PDs with infrared- and visible-blind photoresponse. The heterostructures have been formed by depositing ZnO films on Si(111) substrate with an introduction of AlN as an intermediate layer. The AlN layer helps in improving the crystallinity of the ZnO films and results in excellent optical properties. The vertical transport characteristics of the ZnO/AlN/Si heterojunction-based device under light illumination and in the dark demonstrate an intrinsic infrared- and visible-blind response, with excellent UV responsivity of 14.5 AW^{-1}. The AlN layer acts as an electron blocking layer and allows the holes to get transported across the heterojunction in the reverse biasing condition.

In the past few years, loads of efforts have been made in the field of III-Nitrides/2D materials-based heterostructures for high-performance optoelectronic devices. These 2D materials such as graphene, MoS$_2$, etc. are characterized by weak inter-layer van der Waals (vdW) forces, which lead to exceptional electronic properties, and can offer an open platform to design high-performance electronic devices. Moreover, the absence of surface dangling bonds in 2D materials results in high-quality heterointerfaces. Such an integration has been recently demonstrated by Goel et al. [20], wherein they have shown a high responsivity UV PD based on 2D/3D heterojunction, which has been formed by depositing few-layer of MoS$_2$ on GaN thin film. The superior light absorption properties of MoS$_2$ resulted in high performance MoS$_2$/GaN-based PD. The device shows a high responsivity of 3×10^3 AW^{-1} and detectivity of $\sim 10^{11}$ Jones (at a wavelength of 365 nm) at an applied reverse bias of 1 V under a light intensity of 12 mWcm^{-2}. The rise and the decay times of the PD were 5.3 and 5.6 ms, respectively.

Until now, all the reported devices discussed above require an external applied bias for achieving significant photodetection. In recent times, a lot of efforts are being made towards energy storage and energy producing devices due to the current situation of energy crisis [56–61]. Therefore, PDs that do not consume any external power are gaining a lot of attention. These self-powered devices depend upon the built-in potential at the interface, which enables the effective separation of the photogenerated charge carriers. Additionally, the built-in electric potential lowers the dark current, which is another advantage of such PDs. Thus, these self-powered nanodevices have a great outlook for the next-generation optoelectronic devices.

4.3 III-Nitrides and their heterostructures for self-driven photodetection

Off late, as mentioned above, there has been a tremendous focus on the self-powered PDs. In this section, we emphasize on the various methods unveiled to achieve self-driven photodetection with III-Nitrides-based PDs.

Prakash et al. [62] in 2016 have demonstrated a simple approach to fabricate a self-powered PD utilizing reduced graphene oxide (rGO) asymmetrical electrodes on MBE-grown GaN thin film as shown in **Figure 9(a)**. This integration of the transparent rGO contact electrodes on GaN has been realized through a simple drop-casting method, leading to a simple fabrication process as well as reduced processing time and cost. The hybrid shows a low photoresponsivity of 1.5 μAW^{-1} towards UV light at zero bias (**Figure 9(b)**), with fast response and recovery times of ~60 and ~267 ms, respectively. The difference in the work functions of rGO and GaN leads to formation of depletion regions at the two rGO/GaN interfaces. The drop casted contact electrodes are inhomogeneous in nature, which results into two
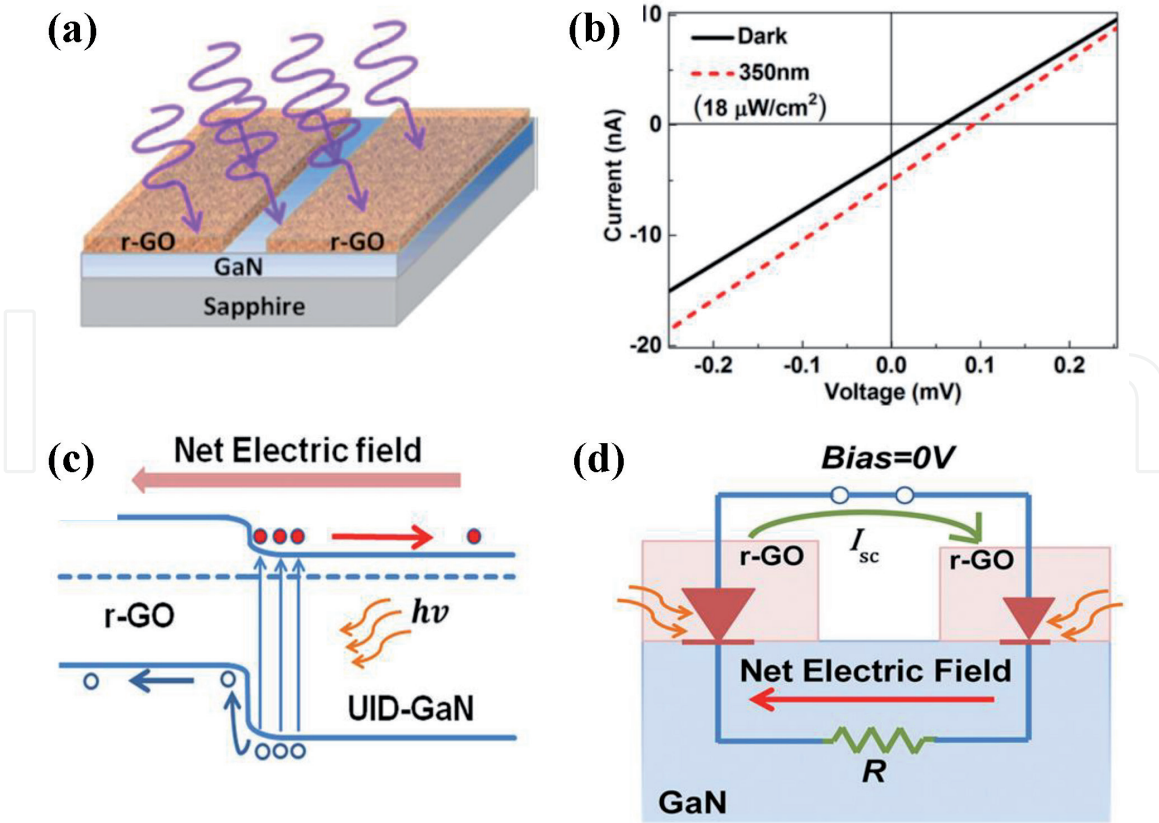
Figure 9.
(a) GaN-based device with rGO electrodes, (b) I-V characteristics of the PD, (c) energy band diagram and (d) mechanism for self-powered photodetection. Figure has been reproduced with permission from Ref. [62].

unlike built-in fields at these interfaces. Therefore, a net internal electric field is developed, leading to the self-powered detection (**Figure 9(c, d)**).

Using the same approach as described above, Pant et al. [63] have reported a self-driven a-GaN-based UV-A PDs showing a responsivity and detectivity of ~4.67 mAW^{-1} and 3.0×10^{13} Jones, respectively at a wavelength of 364 nm. In another work, Aggarwal et al. [64] have shown a UV PD based on GaN nanoflowers grown via MBE on Si(111) substrate. Under self-biased condition, the PD exhibits a very low dark current in the range of $\approx$nA, with a high responsivity of 132 mAW^{-1} and fast rise/fall times of 63/27 ms. In another report, Chowdhury et al. [25] have reported self-powered photodetection of an InN/AlN/Si semiconductor–insulator–semiconductor-based PD (λ = 1550 nm), where a photoresponsivity of ~3.36 μAW^{-1} has been observed with response/recovery times in milliseconds.

The major shortcoming of such devices lies with the obtained responsivities, which is entirely reliant on the degree of inhomogeneity or asymmetry between the electrodes, hence, limiting the PD's performance. One of the most effective ways for realizing self-driven PDs is by fabricating heterojunctions and utilizing the built-in potential at the heterointerface. Heterojunctions of III-Nitrides with several semiconductors such as Si, ZnO, Ga$_2$O$_3$, and so on have been explored and promising results have been achieved. In 2015, the advances in the high growth quality of epitaxial InGaN films on Si substrates synthesized via MBE along with the maturity in the Si-based technology have resulted in the demonstration of highly efficient PDs, as shown by Chandan et al. [65]. A self-powered n-InGaN/n-Si isotype heterojunction-based PD has been reported. The device shows a non-linear behavior and a responsivity of 0.094 AW^{-1}, with rise/fall times less than 100 ms. The mechanism of self-powered photodetection has been explained based on the presence of interfacial internal electric field.

Recently, a high-performance PD based on the p-GaN/n-ZnMgO heterojunction has been demonstrated [24]. The PD shows a clear rectifying *I–V* behavior characterized with a turn-on voltage of ~2.5 V. At zero-bias condition, the device exhibits a responsivity of 196 mAW^{-1} at a wavelength of 362 nm. The rise and the decay times of the PD are as short as 1.7 and 3.3 ms, respectively. This high performance of the device has been attributed to the excellent crystalline quality and electrical properties of p-GaN epilayer.

In another work, a simple approach has been reported [66] to fabricate a GaN/rGO: Ag nanoparticles (NPs) p–n heterojunction-based PD, integrated with a network of transparent Au nanowires (NWs) as the top contact electrode. The device demonstrates an excellent rectification ratio of ~105 with a broad-band photoresponse due to the presence of both the GaN layer (UV region) and the silver-loaded reduced graphene oxide (visible to infrared region). Furthermore, the reducing effect of the Ag NPs to graphene oxide in addition to the localized surface plasmon resonance has been utilized to improve the photoresponse in the NIR and the visible regions. The transparent Au NWs network efficiently collects the charge, ensuing high photoresponsivity and fast switching behavior. The heterojunction exhibits a responsivity of ~266 mAW^{-1} and detectivity of ~2.62 × 10^{11} Jones, under illumination of 360 nm light. Owing to the high built-in electric potential at the heterointerface, the self-powered operation is demonstrated under the entire excitation wavelength range (360–980 nm).

Exploiting the criterion of the difference between the electron affinities of the constituent semiconductors to create an internal field, an improvisation in the InGaN/Si-based structure has been demonstrated by Chowdhury et al. [15], where introduction of an AlN layer in between InGaN and Si leads to the formation of a semiconductor–insulator–semiconductor type structure, resulting in the multifold enhancement in the device performance. The n^+-InGaN/AlN/n-Si(111) hybrid structure has been realized by growing an n^+-InGaN thin film on a commercially obtained AlN/n-Si template using MBE. The device exhibits an exceptional self-powered and broad-band photorespnse under the illumination of UV–visible light (300–800 nm). The self-powered PD exhibits a high responsivity of 9.64 AW^{-1} at light illumination of 580 nm, with an ultrafast response/recovery time of ~20/21 μs, respectively. The maximum response at 580 nm is believed to be because of the deep donor defect states present in the InGaN epilayer.
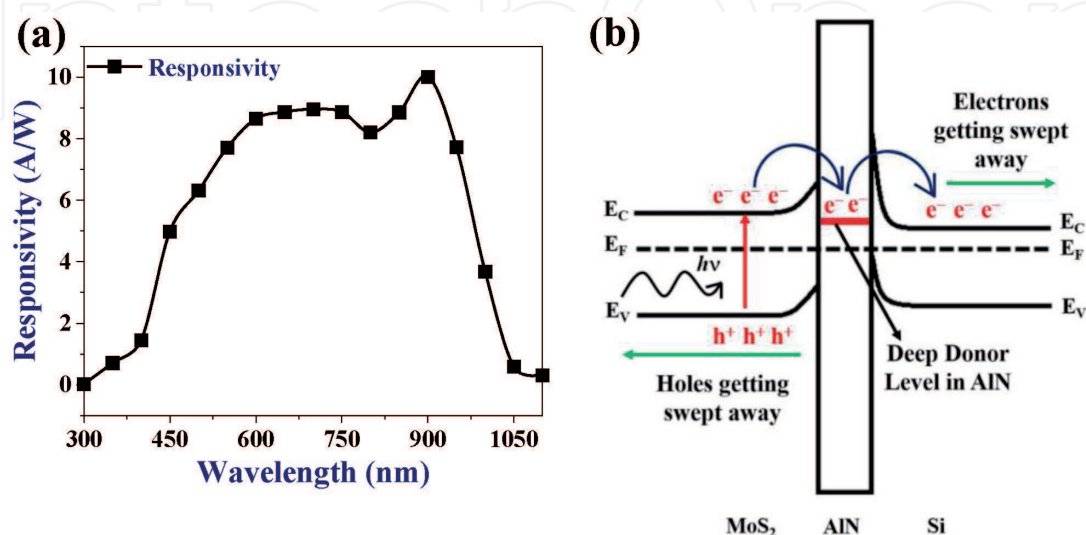
Figure 10.
(a) Spectral response of the MoS$_2$/AlN/Si-based PD. (b) Schematic of the deep defect states-modulated carrier transport in MoS$_2$/AlN/Si-based device. Figures have been reproduced with permission from Ref. [4].

In a recent work, Singh et al. [4] have fabricated an MoS_2/AlN/Si-based PD, combining the mature technologies of III-Nitride and Si with the unique properties of MoS_2. Additionally, due to the large difference between the work functions of these semiconducting materials, the band bending at the heterointerfaces resulted into the self-driven behavior. The vertical transport behavior of the device shows a broad-band photoresponse (300–1100 nm) with maximum responsivity of ~10 AW^{-1} under self-biased condition as shown in **Figure 10(a)**. The device also shows an ultrafast detection speeds (response/recovery times: ~13/15 μs). The importance of sandwiching the AlN layer has been shown as the MoS_2/Si-based PD shows a responsivity ~5 times less in the zero-bias mode. The authors have confirmed through transmission electron microscopy and X-ray photoelectron spectroscopy that oxygen defects exist throughout the AlN layer. These impurities form deep donor levels in AlN and moderate the charge transport, which leads to the enhanced device performance (**Figure 10(b)**).

5. Summary

The last two decades have indisputably witnessed incredible advances in the MBE growth of III-Nitrides and their applications in the area of photodetection. In this chapter, the important concepts about PDs, including the fundamental evaluation parameters and the various sensing mechanisms have been discussed. These mechanisms usually depend on the type of the photoactive material used to fabricate the device. Next, the basic properties of III-Nitrides and the common synthesis techniques used for their production have been reviewed briefly. Finally, a progressive discussion about the PDs based on the III-Nitrides fabricated through MBE has been given and summarized in **Table 1**. These extensive achievements have indisputably established MBE as one of the most reliable methods for fabricating high-quality III-Nitrides and these devices certainly have a lot of potential for the development of the advanced III-Nitrides-based PDs in future.

PD	Bias (V)	Responsivity (mAW^{-1})	Detectivity (Jones)	Rise/Fall Times (ms)
Ag-GaN-Pt [47]	5	633 @ 325 nm (4 mW)	—	—
GaN NS/Si [48]	1	5.7 @ 325 nm (13 mW)	—	—
InN QDs [49]	3	—	—	$1.43×10^3$/ $1.22×10^3$
a-GaN [50]	2	155 @ 360 nm (0.3 mW/cm^2)	—	$6×10^3$/ $15×10^3$
a-GaN [18]	1	$1.9×10^3$ @ 360 nm (0.3 mW/cm^2)	—	210/ $1.2×10^3$
a-GaN [51]	1	$2.5×10^4$ @ 360 nm (0.3 mW/cm^2)	—	222/ $2.1×10^3$
GaN [52]	1	$4.6×10^6$ @ 366 nm	—	—
GaN [53]	15	183 @ 362 nm (0.8 W/m^2)	—	—
GaN/AlN QDs [54]	-1	$2×10^6$ @ 300 nm	—	—
BTO/GaN [21]	5	$4.5×10^4$ @ 350 nm (413 K)	$2.57×10^{12}$	320/220

PD	Bias (V)	Responsivity (mAW^{-1})	Detectivity (Jones)	Rise/Fall Times (ms)
ZnO/AlN/Si [13]	−4	1.45×10^4 @ 365 nm (0.3 mW/cm^2)	—	1.12×10^4/ 7.65×10^4
MoS$_2$/GaN [20]	1	3×10^6 @ 365 nm (12 mW/cm^2)	~10^{11}	5.3/5.6
rGO/GaN [62]	0	1.54 @ 350 nm (18 μW/cm^2)	1.45×10^{10}	60/267
a-GaN [63]	0	4.67 @ 364 nm (0.06 mW/cm^2)	3×10^{13}	50/120
GaN Nanoflowers [64]	0	132 @ 325 nm (13 mW)	2.4×10^{10}	63/27
InN/AlN/Si [25]	0	3.36×10^{-3} @ 1550 nm (106.2 mW/cm^2)	—	10/18
n-InGaN/n-Si [65]	0	94.2 @ 310–380 nm (0.3 mW/cm^2)	—	20/33
p-GaN/n-ZnMgO [24]	0	196 @ 362 nm	—	1.7/3.3
GaN/rGO: Ag NP [66]	0	266 @ 360 nm (0.14 mW/cm^2)	2.62×10^{11}	680/700
InGaN/AlN/Si [15]	0	9.64×10^3 @ 580 nm (0.1 mW/cm^2)	1.93×10^{13}	19.9×10^{-3}/ 21.4×10^{-3}
MoS$_2$/AlN/Si [4]	0	10×10^3 @ 900 nm (0.05 mW/cm^2)	9.39×10^{12}	12.5×10^{-3}/ 14.9×10^{-3}

Table 1.
Comparison of the device performance parameters of various PDs discussed.

6. Outlook

Based upon the analysis of the reported devices in this field, a perspective regarding the future of III-Nitrides-based devices and the related follow-up work have been summarized below:

- The use of transition metal dichalcogenides (TMDCs) as substrates for epitaxial growth of III-Nitrides has been unexplored. TMDCs have a very small lattice mismatch with the III-Nitrides [67], and therefore, high-quality growth can be expected which would result into better device performance.

- The use of 2D transparent materials like graphene, graphene derivatives and 1T phase of TMDCs (semi-metallic), can be used as contact electrodes instead of the conventional metals, as the area for the light absorption gets maximized along with the outstanding electronic properties of these 2D semiconductors.

- Another interesting possibility would be combining non-polar nitrides with layered materials. The absence of the internal polarization field would provide a band to band transition, which is usually absent in the polar devices because of the quantum confined Stark effect at the interfaces. This property is very important for effective photodetection and has been evident from some of the very early works reported on the nonpolar *a*-GaN. Additionally, the presence of anisotropy in electrical conductivity as well as mobility can be helpful in tuning the optoelectronic and electronic properties of the PD.

- Till now, scientists across the world have generally exploited heterojunctions of III-Nitrides with 2D materials in the form of thin films. Heterojunctions based upon the one-dimensional (1D) nanostructures can provide new ways for the development of high-performance optoelectronic devices. The nanorods-based heterointerfaces of the III-Nitrides with 2D materials (growth along these nanorods or a core-shell structure) would enable a much higher aspect ratio and therefore, a much larger area for light absorption as well as a larger active interface, therefore, an enhancement in the optoelectronic performance.

Overall, the excellent properties of the III-Nitride semiconductors make them promising candidates for the applications in photodetection, and these PDs have exhibited outstanding device performance that competes with those available commercially. Thus, III-Nitrides and their heterojunctions-based PDs can be used for the development of futuristic self-biased and ultrafast PDs.

Acknowledgements

Author details

Deependra Kumar Singh[1], Basanta Kumar Roul[1,2], Karuna Kar Nanda[1] and Saluru Baba Krupanidhi[1*]

1 Materials Research Centre, Indian Institute of Science, Bangalore, India

2 Central Research Laboratory, Bharat Electronics, Bangalore, India

*Address all correspondence to: sbkrupanidhi@gmail.com

IntechOpen

References

[1] Wu W, Zhang Q, Zhou X, Li L, Su J, Wang F, et al. Self-powered photovoltaic photodetector established on lateral monolayer MoS_2-WS_2 heterostructures. Nano Energy. 2018;**51**:45-53

[2] Singh RK, Kumar J, Kumar A, Kumar V, Kant R, Singh R. Poly(3-hexylthiophene): Functionalized single-walled carbon nanotubes: (6,6)-phenyl-C61-butyric acid methyl ester composites for photovoltaic cell at ambient condition. Solar Energy Materials and Solar Cells. 2010;94(12):2386-94.

[3] Khan MA, Nanda KK, Krupanidhi SB. Mechanistic view on efficient photodetection by solvothermally reduced graphene oxide. Journal of Material Science: Material in Electronics. 2017;28(19):14818-26.

[4] Singh DK, Pant R, Chowdhury AM, Roul B, Nanda KK, Krupanidhi SB. Defect-Mediated Transport in Self-Powered, Broadband, and Ultrafast Photoresponse of a MoS_2/AlN/Si-Based Photodetector. ACS Applied Electronic Materials. 2020;2(4):944-53.

[5] Mehew JD, Unal S, Torres Alonso E, Jones GF, Fadhil Ramadhan S, Craciun MF, et al. Fast and Highly Sensitive Ionic-Polymer-Gated WS_2-Graphene Photodetectors. Advanced Material. 2017;29:1700222.

[6] Sai Manohar GV, Krupanidhi SB, Nanda KK. Giant enhancement in photoresponse via engineering of photo-induced charge (electron and hole) transfer in linear and non-linear devices. Sensors and Actuators A: Physical. 2020;304:111842.

[7] Ilegems M, Schwartz B, Koszi LA, Miller RC. Integrated multijunction GaAs photodetector with high output voltage. Applied Physics Letters. 1978;33(7):629.

[8] Refaat TF, Abedin MN, Bhagwat V, Bhat IB, Dutta PS, Singh UN. InGaSb photodetectors using an InGaSb substrate for 2μm applications. Applied Physics Letters. 2004;85(11):1874.

[9] Murtaza SS, Campbell JC, Bean JC, Peticolas LJ. Asymmetric dual GeSi/Si Bragg mirror and photodetector operating at 632 and 780 nm. Applied Physics Letters. 1994;65(7):795.

[10] Arora K, Goel N, Kumar M, Kumar M. Ultrahigh performance of self-powered β-Ga_2O_3 thin film solar-blind photodetector grown on cost-effective Si substrate using high-temperature seed layer. ACS Photonics. 2018;5(6):2391-401.

[11] Yao JD, Zheng ZQ, Yang GW. Production of large-area 2D materials for high-performance photodetectors by pulsed-laser deposition. Progress in Materials Science. 2019;106:100573.

[12] Moustakas TD, Iliopoulos E, Sampath AV, Ng HM, Doppalapudi D, Misra M, et al. Growth and device applications of III-nitrides by MBE. Journal of Crystal Growth. 2001;227-228:13-20.

[13] Roul B, Pant R, Chowdhury AM, Chandan G, Singh DK, Chirakkara S, et al. Highly Responsive ZnO/AlN/Si Heterostructure-Based Infrared- and Visible-Blind Ultraviolet Photodetectors With High Rejection Ratio. IEEE Transactions on Electron Devices. 2019;66(3):1345-52.

[14] Mohd Yusoff MZ, Baharin A, Hassan Z, Abu Hassan H, Abdullah MJ. MBE growth of GaN pn-junction photodetector on AlN/Si(111) substrate with Ni/Ag as ohmic contact. Superlattices and Microstructures. 2013;56:35-44.

[15] Chowdhury AM, Chandan G, Pant R, Roul B, Singh DK, Nanda KK,

et al. Self-Powered, Broad Band, and Ultrafast InGaN-Based Photodetector. ACS Applied Material & Interfaces. 2019;11(10):10418-25.

[16] Singh DK, Roul B, Pant R, Chowdhury AM, Nanda KK, Krupanidhi SB. Different types of band alignment at MoS_2/(Al, Ga, In) N heterointerfaces. Applied Physics Letters. 2020;116(25):252102.

[17] Sasaki T, Matsuoka T. Substrate-polarity dependence of metal-organic vapor-phase epitaxy-grown GaN on SiC. Journal of Applied Physics. 1988;64(9):4531-5.

[18] Pant R, Shetty A, Chandan G, Roul B, Nanda KK, Krupanidhi SB. In-plane anisotropic photoconduction in nonpolar epitaxial a-plane GaN. ACS Applied Materials & Interfaces. 2018;10(19):16918-23.

[19] Zhang L, Zhao F, Wang C, Wang F, Huang R, Li Q. Optoelectronic characteristics of UV photodetector based on GaN/ZnO nanorods p-i-n heterostructures. Electronic Materials Letters. 2015;11(4):682-6.

[20] Goel N, Kumar R, Roul B, Kumar M, Krupanidhi SB. Wafer-scale synthesis of a uniform film of few-layer MoS_2 on GaN for 2D heterojunction ultraviolet photodetector. Journal of Physics D: Applied Physics. 2018;51(37):374003.

[21] Pandey BK, Bhat TN, Roul B, Nanda KK, Krupanidhi SB. BTO/GaN heterostructure based on Schottky junction for high-temperature selective ultra-violet photo detection. Journal of Physics D: Applied Physics. 2018;51(4):045104.

[22] Yang W, Hu K, Teng F, Weng J, Zhang Y, Fang X. High-Performance Silicon-Compatible Large-Area UV-to-Visible Broadband Photodetector Based on Integrated Lattice-Matched Type II

Se/n-Si Heterojunctions. Nano Letters. 2018;18(8):4697-703.

[23] Mukhokosi EP, Roul B, Krupanidhi SB, Nanda KK. Toward a fast and highly responsive $SnSe_2$-based photodiode by exploiting the mobility of the counter semiconductor. ACS Applied Materials & Interfaces. 2019;11(6):6184-94.

[24] Zhu Y, Liu K, Ai Q, Hou Q, Chen X, Zhang Z, et al. A high performance self-powered ultraviolet photodetector based on a p-GaN/n-ZnMgO heterojunction. Journal of Materials Chemistry C. 2020;8(8):2719-24.

[25] Chowdhury AM, Pant R, Roul B, Singh DK, Nanda KK, Krupanidhi SB. Double Gaussian distribution of barrier heights and self-powered infrared photoresponse of InN/AlN/Si (111) heterostructure. Journal of Applied Physics. 2019;126(2):025301.

[26] Singh DK, Pant R, Roul B, Chowdhury AM, Nanda KK, Krupanidhi SB. Temperature-Dependent Electrical Transport and Optoelectronic Properties of SnS_2/p-Si Heterojunction. ACS Applied Electronic Materials. 2020;2(7):2155-63.

[27] Gao L, Chen C, Zeng K, Ge C, Yang D, Song H, et al. Broadband, sensitive and spectrally distinctive SnS_2 nanosheet/PbS colloidal quantum dot hybrid photodetector. Light: Science and Applications. 2016;5(7):e16126–e16126.

[28] Ouyang B, Zhao H, Wang ZL, Yang Y. Dual-polarity response in self-powered ZnO NWs/Sb_2Se_3 film heterojunction photodetector array for optical communication. Nano Energy. 2020;68:104312.

[29] Hou Y, Mei Z, Du X. Semiconductor ultraviolet photodetectors based on ZnO and $Mg_xZn_{1-x}O$. Journal of Physics D: Applied Physics. 2014;47(28):283001.

[30] Shkir Mohd, Khan MT, Ashraf IM, Almohammedi A, Dieguez E, AlFaify S. High-performance visible light photodetectors based on inorganic CZT and InCZT single crystals. Scientific Reports. 2019;9(1):12436.

[31] Zhuo R, Wang Y, Wu D, Lou Z, Shi Z, Xu T, et al. High-performance self-powered deep ultraviolet photodetector based on MoS$_2$/GaN p–n heterojunction. Journal of Materials Chemistry C. 2018;6(2):299-303.

[32] Mukhokosi EP, Manohar GVS, Nagao T, Krupanidhi SB, Nanda KK. Device Architecture for Visible and Near-Infrared Photodetectors Based on Two-Dimensional SnSe$_2$ and MoS$_2$: A Review. Micromachines. 2020;11(8):750.

[33] Buscema M, Island JO, Groenendijk DJ, Blanter SI, Steele GA, van der Zant HSJ, et al. Photocurrent generation with two-dimensional van der Waals semiconductors. Chemical Society Reviews. 2015;44(11):3691-718.

[34] Xue F, Yang L, Chen M, Chen J, Yang X, Wang L, et al. Enhanced photoresponsivity of the MoS$_2$-GaN heterojunction diode via the piezo-phototronic effect. NPG Asia Materials. 2017;9(8):e418–e418.

[35] Koppens FHL, Mueller T, Avouris Ph, Ferrari AC, Vitiello MS, Polini M. Photodetectors based on graphene, other two-dimensional materials and hybrid systems. Nature Nanotech. 2014 Oct;9(10):780-93.

[36] Morkoç H. Handbook of nitride semiconductors and devices, Materials Properties, Physics and Growth. John Wiley & Sons; 2009.

[37] Hill, A. Growth, Characterization, and Thermodynamics of III-Nitride Semiconductors. PhD thesis. Arizona State University; 2011.

[38] Maruska HP, Tietjen JJ. The preparation and properties of vapor-deposited single-crystal-line GaN. Applied Physics Letters. 1969;15(10):327-9.

[39] Yoshida S, Misawa S, Gonda S. Improvements on the electrical and luminescent properties of reactive molecular beam epitaxially grown GaN films by using AlN-coated sapphire substrates. Applied Physics Letters. 1983;42(5):427-9.

[40] Pant R, Singh DK, Chowdhury AM, Roul B, Nanda KK, Krupanidhi SB. Next-generation self-powered and ultrafast photodetectors based on III-nitride hybrid structures. APL Materials. 2020;8(2):020907.

[41] Van Hove JM, Hickman R, Klaassen JJ, Chow PP, Ruden PP. Ultraviolet-sensitive, visible-blind GaN photodiodes fabricated by molecular beam epitaxy. Applied Physics Letters. 1997;70(17):2282-4.

[42] Son MS, Im SI, Park YS, Park CM, Kang TW, Yoo K-H. Ultraviolet photodetector based on single GaN nanorod p–n junctions. Materials Science and Engineering: C. 2006;26(5-7):886-8.

[43] Torvik JT, Pankove JI, Van Zeghbroeck BJ. Comparison of GaN and 6H-SiC p-i-n photodetectors with excellent ultraviolet sensitivity and selectivity. IEEE Transactions on Electron Devices. 1999;46(7):1326-31.

[44] Osinsky A, Gangopadhyay S, Yang JW, Gaska R, Kuksenkov D, Temkin H, et al. Visible-blind GaN Schottky barrier detectors grown on Si(111). Applied Physics Letters. 1998;72(5):551-3.

[45] Xu HZ, Wang ZG, Kawabe M, Harrison I, Ansell BJ, Foxon CT. Fabrication and characterization of metal–

semiconductor–metal (MSM) ultraviolet photodetectors on undoped GaN/sapphire grown by MBE. Journal of Crystal Growth. 2000;218(1):1-6.

[46] Calarco R, Marso M, Richter T, Aykanat AI, Meijers R, vd Hart A, Stoica T, Lüth H. Size-dependent photoconductivity in MBE-grown GaN– nanowires. Nano Letters. 2005;5(5):981-4.

[47] Jain SK, Krishna S, Aggarwal N, Kumar R, Gundimeda A, Husale SC, et al. Effect of Metal Contacts on a GaN/Sapphire-Based MSM Ultraviolet Photodetector. Journal of Electronic Materials. 2018;47(10):6086-90.

[48] Goswami L, Pandey R, Gupta G. Epitaxial growth of GaN nanostructure by PA-MBE for UV detection application. Applied Surface Science. 2018;449:186-92.

[49] Shetty A, Kumar M, Roul B, Vinoy KJ, Krupanidhi SB. InN Quantum Dot Based Infra-Red Photodetectors. Journal of Nanoscience and Nanotechnology. 2016;16(1):709-14.

[50] Mukundan S, Roul B, Shetty A, Chandan G, Mohan L, Krupanidhi SB. Enhanced UV detection by non-polar epitaxial GaN films. AIP Advances. 2015;5(12):127208.

[51] Pant RK, Singh DK, Roul B, Chowdhury AM, Chandan G, Nanda KK, et al. Photodetection Properties of Nonpolar a-Plane GaN Grown by Three Approaches Using Plasma-Assisted Molecular Beam Epitaxy. Physica Status Solidi A. 2019;216(18):1900171.

[52] Wang X, Wang X, Wang B, Xiao H, Liu H, Wang J, et al. High responsivity ultraviolet photodetector based on crack-free GaN on Si (111). Physica Status Solidi A. 2007;4(5):1613-6.

[53] Ravikiran L, Radhakrishnan K, Dharmarasu N, Agrawal M,

Wang Z, Bruno A, et al. GaN Schottky Metal–Semiconductor–Metal UV Photodetectors on Si(111) Grown by Ammonia-MBE. IEEE Sensors Journal. 2017;17(1):72-7.

[54] Rigutti L, Tchernycheva M, De Luna Bugallo A, Jacopin G, Julien FH, Zagonel LF, et al. Ultraviolet Photodetector Based on GaN/AlN Quantum Disks in a Single Nanowire. Nano Letters. 2010;10(8):2939-43.

[55] Mohd Yusoff MZ, Mahyuddin A, Hassan Z, Abu Hassan H, Abdullah MJ, Rusop M, et al. AlN/GaN/AlN heterostructures grown on Si substrate by plasma-assisted MBE for MSM UV photodetector applications. Materials Science in Semiconductor Processing. 2015;29:231-7.

[56] Wu Y, Yu Y. 2D material as anode for sodium ion batteries: Recent progress and perspectives. Energy Storage Materials. 2019;16:323-43.

[57] Li X, Wu J, Mao N, Zhang J, Lei Z, Liu Z, et al. A self-powered graphene–MoS$_2$ hybrid phototransistor with fast response rate and high on–off ratio. Carbon. 2015;92:126-32.

[58] Kumar A, Singh RK, Singh HK, Srivastava P, Singh R. Enhanced capacitance and stability of p-toluenesulfonate doped polypyrrole/carbon composite for electrode application in electrochemical capacitors. Journal of Power Sources. 2014;246:800-7.

[59] Kumar A, Singh HK, Singh RK, Singh R, Srivastava P. P-toluenesulfonate doped polypyrrole/carbon composite electrode and a process for the preparation thereof. United States patent US 10,074,453. 2018.

[60] Rambabu A, Singh DK, Pant R, Nanda KK, Krupanidhi SB. Self-powered, ultrasensitive, room

temperature humidity sensors using SnS_2 nanofilms. Scientific Reports. 2020;10(1):14611.

[61] Kumar S, Faraz M, Khare N. Enhanced thermoelectric properties of Sb_2Te_3-graphene nanocomposite. Materials Research Express. 2019;6(8):085079.

[62] Prakash N, Singh M, Kumar G, Barvat A, Anand K, Pal P, et al. Ultrasensitive self-powered large area planar GaN UV-photodetector using reduced graphene oxide electrodes. Applied Physics Letters. 2016;109(24):242102.

[63] Pant R, Singh DK, Chowdhury AM, Roul B, Nanda KK, Krupanidhi SB. Highly Responsive, Self-Powered *a* -GaN Based UV-A Photodetectors Driven by Unintentional Asymmetrical Electrodes. ACS Appl Electronic Materials. 2020;2(3):769-79.

[64] Aggarwal N, Krishna S, Sharma A, Goswami L, Kumar D, Husale S, et al. A Highly Responsive Self-Driven UV Photodetector Using GaN Nanoflowers. Advanced Electronic Materials. 2017;3(5):1700036.

[65] Chandan G, Mukundan S, Mohan L, Roul B, Krupanidhi SB. Trap modulated photoresponse of InGaN/Si isotype heterojunction at zero-bias. Journal of Applied Physics. 2015;118(2):024503.

[66] Sarkar K, Hossain M, Devi P, Rao KDM, Kumar P. Self-Powered and Broadband Photodetectors with GaN: Layered rGO Hybrid Heterojunction. Advanced Materials Interfaces. 2019;6(20):1900923.

[67] Gupta P, Rahman AA, Subramanian S, Gupta S, Thamizhavel A, Orlova T, et al. Layered transition metal dichalcogenides: promising near-lattice-matched substrates for GaN growth. Scientific Reports. 2016;6(1):23708.